

# Measurements of rate constants of O<sub>2</sub>(b) quenching by CH<sub>4</sub>, NO, N<sub>2</sub>O at temperatures 300-800 K

*G.I. Tolstov*<sup>1,2\*</sup>, *M.V. Zagidullin*<sup>1,2</sup>, *N.A. Khvatov*<sup>1,2</sup>, *I.A. Medvedkov*<sup>1,2</sup>, *A.M. Mebel*<sup>1,3</sup>,  
*M.C. Heaven*<sup>1,4</sup> and *V.N. Azyazov*<sup>1,2</sup>

<sup>1</sup>Samara University, Samara, 443086, Russia

<sup>2</sup>Lebedev Physical Institute of RAS, Samara, 443011, Russia

<sup>3</sup>Florida International University, Miami, 33199, USA

<sup>4</sup>Emory University, Atlanta, Georgia 30322, USA

**Abstract.** Electronically excited oxygen has an important place in the kinetic schemes of the processes taking place in the atmosphere, in the active medium of an oxygen-iodine laser, and in plasma-assisted combustion<sup>1</sup>. Over the past decades, a large amount of data on the rate constants of quenching O<sub>2</sub>(b) on a large number of collision partners has been accumulated. However, they mostly refer to the results of measurements at room temperature. In this paper, rate constants for the quenching of O<sub>2</sub>(b) by collisions with N<sub>2</sub>O, NO, and CH<sub>4</sub> have been determined in the temperature range from 297 to 800 K, by the laser-induced fluorescence method. O<sub>2</sub>(b) was excited by pulses from a tunable dye laser, and the deactivation kinetics were followed via observing the temporal behavior of the b<sup>1</sup>Σ<sub>g</sub><sup>+</sup> → X<sup>3</sup>Σ<sub>g</sub><sup>-</sup> fluorescence. From the analysis of experimental results, the following temperature dependencies of the quenching rate constants by these gases were obtained, and could be represented by the expressions:  $k_{\text{NO}} = (1.77 \pm 0.2) \times 10^{-24} \times T^{3.5} \exp(1138 \pm 37/T)$ ;  $k_{\text{N}_2\text{O}} = (2.63 \pm 0.14) \times 10^{-16} \times T^{1.5} \times \exp(590 \pm 26/T)$  and  $k_{\text{CH}_4} = (3.54 \pm 0.4) \times 10^{-18} \times T^{1.5} \times \exp(-220 \pm 24/T)$  cm<sup>3</sup>s<sup>-1</sup>. All of the rate constants measured at room temperature were found to be in good agreement with previously reported values.

## 1 Introduction

Gas phase processes with oxygen molecules in second electronically excited state b<sup>1</sup>Σ<sub>g</sub><sup>+</sup> has been studied extensively in last decades, due to the importance of these processes in the terrestrial atmosphere [1-3], oxygen-containing gas discharges [4-6] and combustion [7-10]. Plasma-chemicals processes in the air-fuel mixtures result in formation of O<sub>2</sub>(b<sup>1</sup>Σ<sub>g</sub><sup>+</sup>) molecules that may activates chain reactions in the combustion zones [11]. Analysis of

---

\* Corresponding author: [outlook@yandex.ru](mailto:outlook@yandex.ru)

reaction kinetics involving  $O_2(b^1\Sigma_g^+)$  is made difficult, because there is little published data concerning the deactivation kinetics at temperatures above 350 K.

Studies of the  $O_2(b^1\Sigma_g^+)$  deactivation at room temperature by molecules relevant to combustion are represented by many works:  $CH_4$  [12-17],  $NO$  [18],  $N_2O$  [12,13,18-20]. So, the aim of this work was to determine the rate constants for removal of  $O_2(b^1\Sigma_g^+)$  by the  $CH_4$ ,  $NO$ , and  $N_2O$  molecules at temperatures up to  $\sim 800K$  using time-resolved emission from the  $O_2\ b^1\Sigma_g^+ - X^3\Sigma_g^-$  transition.

## 2 Experiment

The measurements were made by observing the decay profiles of emission intensity from excited oxygen  $O_2(b^1\Sigma_g^+)$  on the addition to the oxygen flow of the quencher, using the excitation of  $b^1\Sigma$  state by pulsed dye laser. An oxygen-quencher gas mixture flowed through the fluorescence cell (FC), which consisted of a cylindrical quartz tube 40 cm long, with an internal diameter of 15 mm, the ends were sealed by quartz windows, mounted at an angle. The oxygen-containing mixture was prepared right before the entrance to the FC. The mixture was heated via the heat transfer from the warmed walls of the quartz tube. The temperature of the walls was maintained by resistive heating of the nichrome tape wound on it and the corresponding thermal insulation. To observe emission from  $O_2(b^1\Sigma_g^+)$  a rectangular window, 2 cm long and 1 cm high was located in the center of FC. This aperture was free of insulating materials and heating tape. The gases used had the following minimum purities stated by the manufacturers:  $O_2(>99.99995)$ ,  $CH_4 (>99.99\%)$ ,  $N_2O (>99.8\%, H_2O<0.025\%)$ ,  $NO, (>99.9\%)$  were used in the experiments. The gas temperature in the LIF region was measured by a thermocouple.

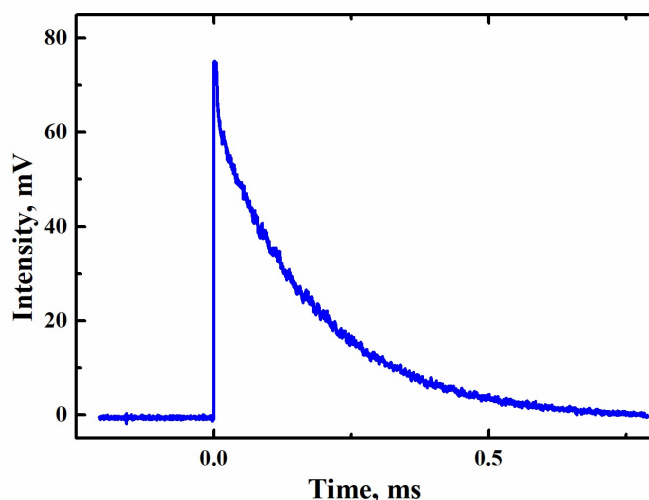


**Fig. 1.** Temporal profiles of the  $O_2(b)/CH_4$  mixture recorded for oxygen partial pressure  $P_{O_2} = 657.3$  Torr, and  $CH_4$  number density  $n_{CH_4} = 4.11 \times 10^{-16} \text{ cm}^{-3}$  at gas temperature  $T = 300K$

The dye laser beam (Sirah Precision Scan, PSCAN-D-18-EG) was directed along the central axis of the FC. This laser pulse excited oxygen molecule into  $(b^1\Sigma_g^+, v=1)$  state. In excess  $O_2(X)$ , the  $O_2(b^1\Sigma_g^+, v=1)$  was rapidly transferred to  $O_2(b^1\Sigma_g^+, v=0)$  by efficient E-E and V-V energy-exchange processes[21]. Oxygen  $^1\Sigma_g^+, v=0 \rightarrow ^3\Sigma_g^-, v=0$  emission was

observed through the window in FC, along an axis that was perpendicular to the dye laser beam. The light was collected and focused on the entrance slit of a monochromator (MDR-206), transmitting wavelengths in the  $762 \pm 8$  nm range. Additional long-pass filters were used to suppress the scattered radiation at 690 nm. Time-resolved LIF signals were recorded using a PMT (Hamamatsu R636-10). To measure time resolved fluorescence decay curves, the PMT output electric signals stored in memory of digital oscilloscope (LeCroy Wavesurfer-3054R).

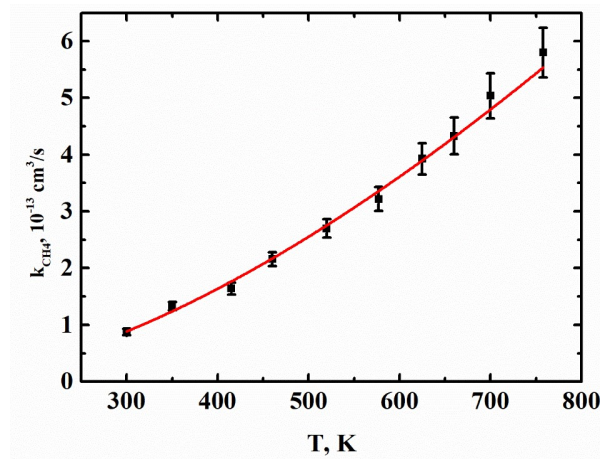


**Fig. 2.** Rate constant  $k_{CH_4}$  as a function of temperature. Solid curve is the plot of  $3.54 \times 10^{-18} T^{1.5} \exp(-220/T)$ .

### 3 Results

The PMT response temporal profile shown on Figure 1 have bi-exponential behavior due to the instrumental decay caused by short (10 ns) scattering emission and the decay of  ${}^1\Sigma_g^+ \rightarrow {}^3\Sigma_g^-$  emission. The decay of these profile can be fitted by two exponents:  $A_0 + A_r \exp(-K_r t) + A \exp(-Kt)$ , where  $(1/K_r)$  is the instrumental response time of the order of  $2\mu\text{s}$ . The decay rate of  $O_2({}^1\Sigma_g^+)$  removal  $K$  in the processes



is given by expression

$$K = k_{O_2} n_{O_2} + k_M n_M, \quad (3)$$

where  $n_{O_2}$  and  $n_M$  are the number densities of oxygen  $O_2$  and an admixed gas M,  $k_{O_2}$  and  $k_M$  are rate constants of processes (1) and (2) respectively. Application of the ideal gas approximation yields the expression [22]

$$k_m = K \left( \frac{k_B T}{P} \right) \frac{G}{G_{O_2}},$$

where

$$k_m = k_{O_2} + \frac{G_M}{G_{O_2}} k_M \quad (4)$$

is the combined rate coefficient. Here  $P$  is the gas pressure,  $T$  is the gas temperature,  $k_B$  is the Boltzmann constant,  $G$  is the total flow rate,  $G_M$  is the flow rate of the admixed gas M.

The plot of  $k_m$  versus  $G_M/G_{O_2}$  for flowing gas is the analogues to the Stern-Folmer plot of  $K$  versus number density of M for static condition. The slope of linear fit according to equation (4) gives rate constant  $k_M$ . Then the set of data of  $k_M$  vs  $T$  was fitted according to equation

$$k_M(T) = AT^{0.5n} \exp(-E/T) \quad (5)$$

with integer value for  $n$  was used to obtain analytical temperature dependence of rate constants.

We observed that the temperature of the gas mixture in the LIF observation region, directly opposite the center of the fluorescence observation window, was somewhat lower than the upstream or downstream temperatures. The temperature gradient was present because the higher heat transfer through the window in the wall of the quartz tube. Temperature variations were taken into account in estimating the measurement errors.

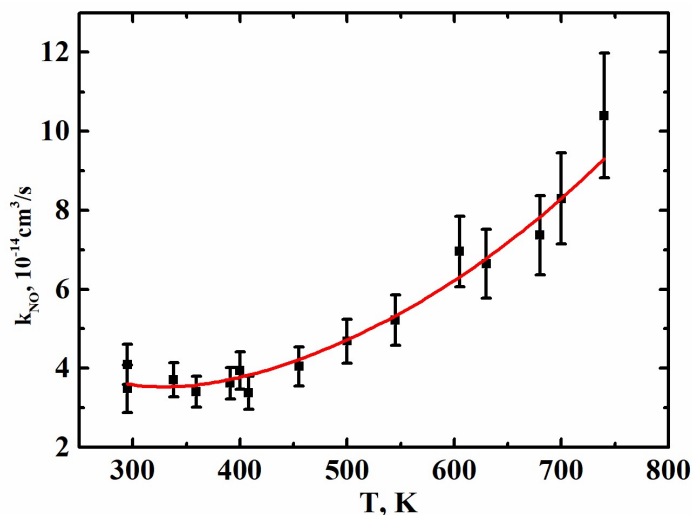


**Fig. 3.** Rate constant  $k_{NO}$  as a function of temperature. Solid curve is the plot of  $1.77 \times 10^{-24} \times T^{3.5} \exp(1138/T)$  fitting experimental data (symbols). The results of measurements (symbols) and plots of equations for  $k_M(T)$  for removal species are shown in Figures 2-4.

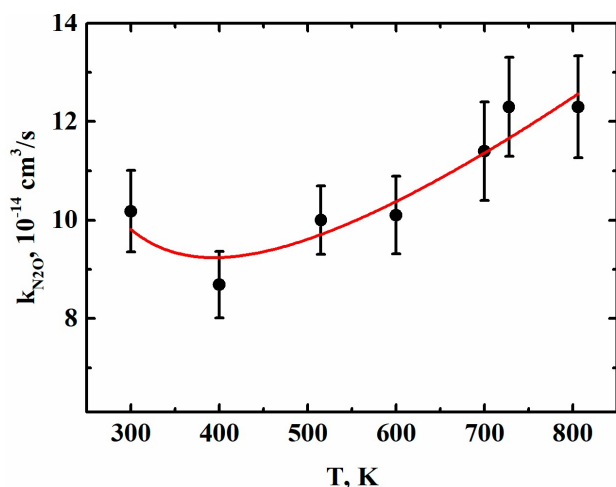


**Fig. 4.** Rate constant  $k_{N2O}$  as a function of temperature. Solid curve is the plot of  $2.63 \times 10^{-18} T^{1.5} \exp(590/T)$  fitting experimental data (symbols).

## 4 Conclusion

The measured values of the rate constants for room temperature are in good agreement with the results of other studies. For each of the collisional partners M the fitting expression of the type (5) was derived in the temperature range 297-800 K. The measured values of the rate constants and fitting expressions for  $k_M(T)$  can be used in modeling of the gas kinetics processes involved  $O_2(b^1\Sigma_g^+)$  molecules in the temperature range 297-800 K.

This work was supported by the Ministry of Education and Science of the Russian Federation under the Grant No. 14.Y26.31.0020 to Samara University.

## References

1. T.G. Slanger, R.A Copeland, *Chem. Rev.* **103** (2003).
2. A.S. Kirillov, *Chem. Phys.*, **410** (2013).
3. V.A. Krasnopolsky, *Planetary and Space Science*, **59**, (2011).
4. G. Nayak, J.S. Sousa, P.J. Bruggeman, *Journal of Physics D: Applied Physics*, **50**, (2017).
5. T. Wegner, C. Küllig, J. Meichsner, *Plasma Sources Science and Technology*, **26**, (2017).
6. Y.A. Mankelevich, E.N. Voronina, A.Y. Poroykov, T.V. Rakhimova, D.G. Voloshin, A.A. Chukalovsky, *Plasma Physics Reports*, **42**, (2016).
7. A.M. Starik, A.V. Pelevkin, N.S. Titova, *Combustion and Flame*, **176**, (2017).
8. A.A. Konnov, *Combustion and Flame*, **162**, (2015).
9. L.V. Bezgin, V.I. Kopchenov, A.M. Starik, N.S. Titova, *Combustion, Explosion, and Shock Waves*, **53**, (2017).
10. A.V. Pelevkin, B.I. Loukhovitski, A.S. Sharipov, *The Journal of Physical Chemistry A*, **121**, (2017).
11. A. Starik, A. Sharipov, *Physical Chemistry Chemical Physics*, **13**, (2011).
12. S.V. Filseth, A. Zia, K.H. Welge, *J.Chem.Phys.*, **52**. (1970).
13. K.H. Becker, W. Groth, U. Schurath, *Chem.Phys.Lett.*, **8**, (1971).
14. J. Wildt, G. Bednarek, E.H. Fink, R.P. Wayne, *Chem. Phys.*, **122**, (1988).
15. K. Kohse-Höinghaus, F. Stuhl, *J. Chem. Phys.*, **72**, (1980).
16. J.A. Davidson, E.A. Ogryzlo, *Can. J. Chem.*, **52**, (1970).
17. E.J. Dunlea, R.K. Talukdar, A.R. Ravishankara, *J. Phys. Chem. A*, **109**, (2005).
18. R. Boodaghians, P. Borrell, P. Borrell, *Chem.Phys.Lett.*, **97**, (1983).
19. P.M. Borrell, P. Borrell, K.R. Grant, *The Journal of Chemical Physics* **78**, (1983).
20. E.J. Dunlea, R.K. Talukdar, A.R. Ravishankara, *Zeitschrift für Physikalische Chemie.*, **224**, (2010).
21. H.I. Bloemink, R.A. Copeland, T.G. Slanger. *J. Chem. Phys.*, **109**, (1998).
22. M.V. Zagidullin, N.A. Khvatov, I.A. Medvedkov, G.I. Tolstov, A.M. Mebel, M.C. Heaven, V.N. Azyazov, *J. Phys. Chem. A*, **121**, (2017).